Glycative Stress Research

Online edition : ISSN 2188-3610
Print edition : ISSN 2188-3602
Received : January 8, 2025
Accepted : February 27, 2025
Published online : March 31, 2025
doi:10.24659/gsr.12.1_25

*Original article*

# Extracellular vesicles from probiotic microorganisms enhance microglia amyloid β phagocytosis

Kyle Haasbroek [1)], Shino Otaka [2)], Chieko Sakiyama [1)], Shohei Iwase [3)], Masayuki Yagi [1)], Yoshikazu Yonei [1)]

1) Anti-Aging Medical Research Center/Glycative Stress Research Center, Graduate School of Life and Medical Sciences, Doshisha University, Kyoto, Japan
2) Sapporo Division, Cosmo Bio Co., Ltd., Otaru, Hokkaido, Japan
3) Drug Discovery and Contract Services Division, Cosmo Bio Co., Ltd., Tokyo, Japan

## Abstract

Microglia phagocytotic activity is vital for homeostasis of the brain by clearing waste, debris, and insoluble aggregates of amyloid β (Aβ) and other proteins. Genetic predisposition is an important factor in the etiology of Alzheimer's disease (AD), with mutations in genes regulating microglia function and phagocytosis strongly associated with AD risk. However, factors such as lifestyle (*e.g.*, smoking), systemic processes (*e.g.*, glycative and oxidative stresses), and dysbiosis of the intestinal and oral microbiomes have also been implicated in the pathogenesis of neurodegenerative diseases. Mesenchymal stem cell secretome has shown promise as a treatment to improve microglia phagocytosis and cognitive function, while conversely pathogenic bacterial molecular patterns (putatively transmitted by extracellular vesicles [EVs]) are suspected to promote neurodegeneration. In this study, we used our recently developed Aβ phagocytosis model to examine the effects of EVs from probiotic microorganisms on phagocytotic capacity of BV2 microglia. Among the bacterial and yeast strains tested, EVs from *Bacillus coagulans* lilac-01 and *Escherichia coli* DH5α both induced a substantial increase in Aβ uptake in a dose dependent manner. As EVs are capable of crossing the blood brain barrier and directly interact with microglia, probiotic EVs have great potential as a treatment for improving microglia functioning in AD and other neurodegenerative diseases.

***KEY WORDS*:** microglia, amyloid β, phagocytosis, dementia, microbiota, extracellular vesicles

## Introduction

Microglia are the resident immune cells of the central nervous system (CNS) whose role is to monitor the CNS environment, clear waste and debris, and enact immune responses to injury and infection. Microglia phagocytosis critically maintains the CNS environment by clearing and breaking down waste, debris, and insoluble aggregates. Alzheimer's disease (AD) and other neurodegenerative disorders are associated with a built up of neurotoxic plaques, particularly those consisting of Tau and amyloid beta (Aβ). As microglia phagocytosis is indispensable for the clearing of Aβ aggregates, microglia function has been implicated as an important factor in the pathogenesis of age-associated neurodegenerative processes. On the other hand, overactivation of microglia leads to a neurotoxic inflammatory response and pathogenic phagocytosis of neuronal and synaptic components near plaques. Proper microglia functioning may be the key to the prevention of neurodegenerative diseases.

While the genetic causes of autosomal dominant AD involve mutations in Aβ precursor genes presenilin 1 and 2, the genetic factors of late-onset AD (which comprises 90% of AD cases) are much less clear. Nevertheless, many genes that are associated with late-onset AD are enriched in microglia and key risk genes heavily involve phagocytosis regulators and receptors[1-3)]. Mutations in genes such as TREM2, CD33, ABCA7, MS4A6A, and APOE inhibit phagocytosis and impair Aβ clearance. The phagocytosis capacity of microglia is vital for preventing neurodegeneration.

Additionally, dysbiosis of the human microbiomes

Correspondence to: Professor Yoshikazu Yonei, MD, PhD
Anti-Aging Medical Research Center/Glycative Stress Research Center,
Graduate School of Life and Medical Sciences, Doshisha University
1-3, Tatara Miyakodani, Kyotanabe, Kyoto, 610-0394 Japan
TEL & FAX: +81-774-65-6394 e-mail: yyonei@mail.doshisha.ac.jp
Co-authors: Haasbroek K, kylehaasbroek@gmail.com;
Otaka S, shino-otaka@cosmobio.co.jp; Sakiyama C, csakiyam@mail.doshisha.ac.jp;
Iwase S, shohei-iwase@cosmobio.co.jp; Yagi M. myagi@mail.doshisha.ac.jp

has also been implicated to play a contributary role in neurodegenerative disease. Intestinal dysbiosis[4,5] and increased intestinal permeability[6-8] are correlated with various forms of cognitive impairment, and microbiome composition has been characterized in association with all-cause dementia[9] and AD[10,11]. Neurological damage is also a common effect observed in elderly patients following recovery from sepsis[12], and even induces Aβ accumulation in the brain[13]. Bacterial endotoxins, such as lipopolysaccharide (LPS), are significantly elevated in the blood of patients with neurodegenerative disease[14,15] causing systemic inflammation[16] which exacerbates systemic contributors to AD such as oxidative and glycative stress. Recently, genetic material belonging to the bacterium *P. gingivalis*, the causative pathogen of gingivitis, was discovered in AD brains[17], and periodontitis has been reported to correlate with AD, but not other causes of dementia[18].

While the mechanism of the connection between bacterial dysbiosis and cognitive decline remains to be clarified, it has been speculated that extracellular vesicles (EVs) produced by bacteria may be the answer. EVs are able to pass through the intestinal epithelium and reach tissues throughout the body[19]. Bacterial EVs have been observed in the blood of healthy people[20] and are mainly derived from intestinal microbiota. There is a significant increase in blood bacterial EV concentrations in populations older than 55 years of age[21] that is likely due to increased intestinal permeability[22]. EVs are also be able to penetrate the blood brain barrier (BBB)[23]. In addition to immunomodulation induced by surface moieties interacting with host receptors, EVs also carry myriad nucleic acids, lipids, and proteins as cargo that may influence target cells. Bacterial EVs are taken up into host cells[24], although the mechanism remains unclear. Phagocytosis, various endocytosis pathways, and direct membrane fusion are all possible mechanisms[25].

The potential effects of bacterial EVs are numerous and varied. Gram type, species, strain, and environmental conditions may greatly influence the content, size, and phenotype of EVs produced by a cell. Due to their ability to pass the BBB, EVs may be the physical link between external bacteria and the CNS environment. Host EVs act as signals that can alter the behavior of microglia. In a previous phase of this research EVs produced by mesenchymal stem cells enhanced microglia Aβ phagocytosis[26]. Further, the mesenchymal stem cell secretome has been shown to improve cognitive functioning in AD when administered via nasal spray[27-29]. It has been similarly speculated that EVs produced by bacteria and other microorganisms could be utilized for neuroprotective purposes. Bacterial EVs can have various immunomodulatory effects dependent on their type[30]. EVs from probiotic species have shown anti-inflammatory effects[31,32], while pathogenic EVs can enhance inflammation[33,34]. We predict that probiotic EVs will ameliorate microglia-phagocytosis-mediated neurodegenerative disease. In this study, EVs from several probiotic bacteria and yeast were tested in an *in vitro* Aβ phagocytosis model using murine BV2 microglia cells to evaluate their effectiveness in improving microglia phagocytic activity.

## *Methods*

### *Microglia cell line*

In order to maintain stability of results over a large number of samples and repeated experiments, mouse microglia cell line BV2 (Code No.: 305156-Academic, Cell Lines Service GmbH, Germany) was used in this study. Such cell lines have a precedence of use for evaluation of Aβ phagocytosis[35]. BV2 cell cultures were prepared using RPMI 1640 medium (Thermo Fisher Scientific Inc.) with 10% fetal bovine serum (FBS) and Penicillin-Streptomycin (Fujifilm Wako Pure chemicals) at 100 IU/mL (0.1 mg/mL). During fluorescence imaging, phenol red-free RPMI 1640 medium (Thermo Fisher Scientific Inc.) with 10% FBS and Penicillin-Streptomycin (100 IU/mL) was used.

### *Aβ synthesis and pretreatment*

TAMRA-labeled mouse Aβ (1-42) was synthesized by the Peptide Unit of Cosmo Bio. The sequence was 5-TAMRA-XDAEFGHDSGFEVRHQKLVFFAEDV GSNKGAIIGLMVGGVVIA X:AEEAc (PEG), with a molecular weight of 4975.57 g/mol. Aβ was dissolved in trifluoroacetic acid (TFA, Nacalai Tesque) to a concentration of 1 mg/mL. 100 µL aliquots were diluted 10-fold in distilled water in pairs of microtubes before drying via centrifugal evaporation. Aβ aggregates were loosened with 100 µL per tube of 1,1,1,3,3,3-hexafluoro-2-propanol (HFIP, Kanto Kagaku) before being redissolved and dried once more with centrifugal evaporation before storage at –20 °C.

Aβ samples were prepared for experimentation the day before cell addition. Dried Aβ was dissolved in 40 µL of dimethyl sulfoxide (DMSO, Merck KGaA), resulting in a 2.5 mg/mL solution. This was further diluted 25-fold with 960 µL of growth medium. resulting in a final concentration of 100 µg/mL (20 µM) Aβ and 4% DMSO. Aβ medium was incubated at 4 °C for 24 hours to oligomerize the Aβ.

### *Extracellular vesicles (EVs)*

Microorganism EVs (Cosmo Bio) derived from probiotic strains of lactic acid bacteria, *E. coli*, and yeast were procured and applied to microglia cultures over a range of concentrations (1%, 0.1%, and 0.01% v/v). EVs from the following strains were utilized for testing: *Bacillus coagulans* lilac-01 (LBEV01), *Leuconostoc mesenteroides* 180720-12-1 (LBEV-R1), *Lactobacillus paracase*i 180913-R1 (LBEV-R2), *Escherichia coli* DH5α (ECEV), *Hanseniaspora vineae* 181019Y5-2 (YSEV-R3), *Kloeckera apiculata* 180926-3 (YSEV-R4), *Saccharomyces cerevisiae* 164-4 (YSEV-R5), and *Saccharomyces paradoxus* 181211-12 (YSEV-R6).

### *Experimental procedure: Aβ phagocytosis*

BV2 cells were cultured to reach a sufficient volume via passaging. Cells were seeded in 96-well plates at a density of $5x10^3$ cells/well. One day after seeding, 100 µL of medium was added to each well of the following compositions:

| Control Samples | | |
|---|---|---|
| Negative control | Aβ: None | DMSO: 0.2% |
| Positive control | Aβ: 1 μM | DMSO: 0.2% |

| Bacteria and Yeast EVs | | | |
|---|---|---|---|
| ×100 | Aβ: 1 μM | DMSO: 0.2% | EV: 1% |
| ×1,000 | Aβ: 1 μM | DMSO: 0.2% | EV: 0.1% |
| ×10,000 | Aβ: 1 μM | DMSO: 0.2% | EV: 0.01% |

Following 24-hours of incubation the supernatant was removed and wells were washed with HBSS (-), and 100 μL of phenol red-free medium was added. Cells were imaged with an all-in-one microscope (BZX-710, Keyence), collecting both phase-contrast and TAMRA-Aβ fluorescence images. Image analysis was conducted to calculate the total area of the cells and the fluorescence intensity of each image. An example of the images collected for analysis is demonstrated in ***Fig. 1***. Fluorescence intensity was corrected according to the following formula:

(TAMRA fluorescence intensity) / (total cell area) = fluorescence intensity per unit area

The value of each sample group was normalized to the negative control group (% NC) and positive control group (% Aβ) of each plate.

## *Results*

Mouse BV2 microglia were treated with media containing 1 μM Aβ and probiotic EVs over a range of dilutions (x100, x1,000, x10,000). After incubation, culture wells were washed and clean media was exchanged before fluorescence analysis. Representative images of each sample group are collected in ***Fig. 2***. Fluorescent TAMRA-Aβ taken up by microglia was measured in order to evaluate the effects of EVs on Aβ phagocytosis. The results are depicted in ***Fig. 3***. as a percentage Aβ uptake in relation to positive control samples. Each sample group was normalized to the relevant control samples cultured together on the same plate. The full measurement data for each plate and sample group are shown in ***Tables 1-4***.

Among the test samples, those treated with EVs from *B. coagulans* lilac-01 EVs (LBEV-01) and *E. coli* DH5α EVs (ECEV) demonstrated strong dose-dependent increases in Aβ phagocytosis. LBEV-01 treatments at a 100-times dilution were measured at 277% of control, 188% at 1,000-times dilution, and approached baseline with 102% at 1,000-times dilution. ECEV treated microglia enhanced Aβ phagocytosis to 712%, 497%, and 353% at dilutions of 100, 1,000, and 10,000-times respectively.

Yeast EV treatments exhibited weak and inconsistent effects. *Hanseniaspora* vineae EVs (YSEV-R3) inhibited Aβ phagocytosis at all dosages, reaching 50% of control at a dilution of 10,000-times. *Saccharomyces paradoxus* EVs (YSEV-R6), conversely, increasingly enhanced phagocytosis at lower concentrations, to a maximum of 150% of control at 10,000-times dilution.

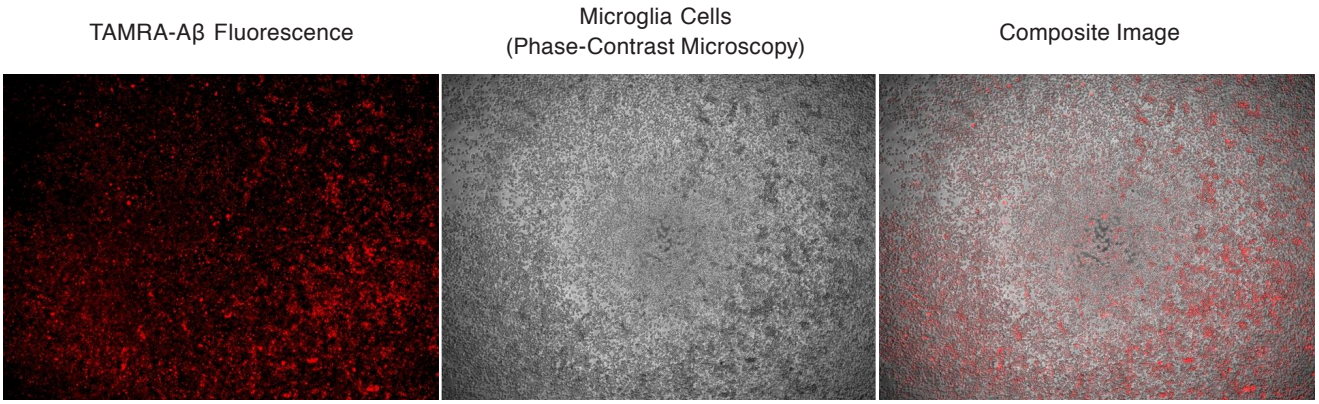


***Fig. 1.*** **Fluorescence measurement methodology demonstration.**
On the left is a fluorescence microscopy image of TAMRA-tagged Aβ in red, used to measure total fluorescence of each sample well. In the center is the phase-contrast image of microglia which was used to measure total cell area. On the right is a composite image. Fluorescence intensity per unit area was calculated by dividing measured fluorescence by total cell area.

**a)**

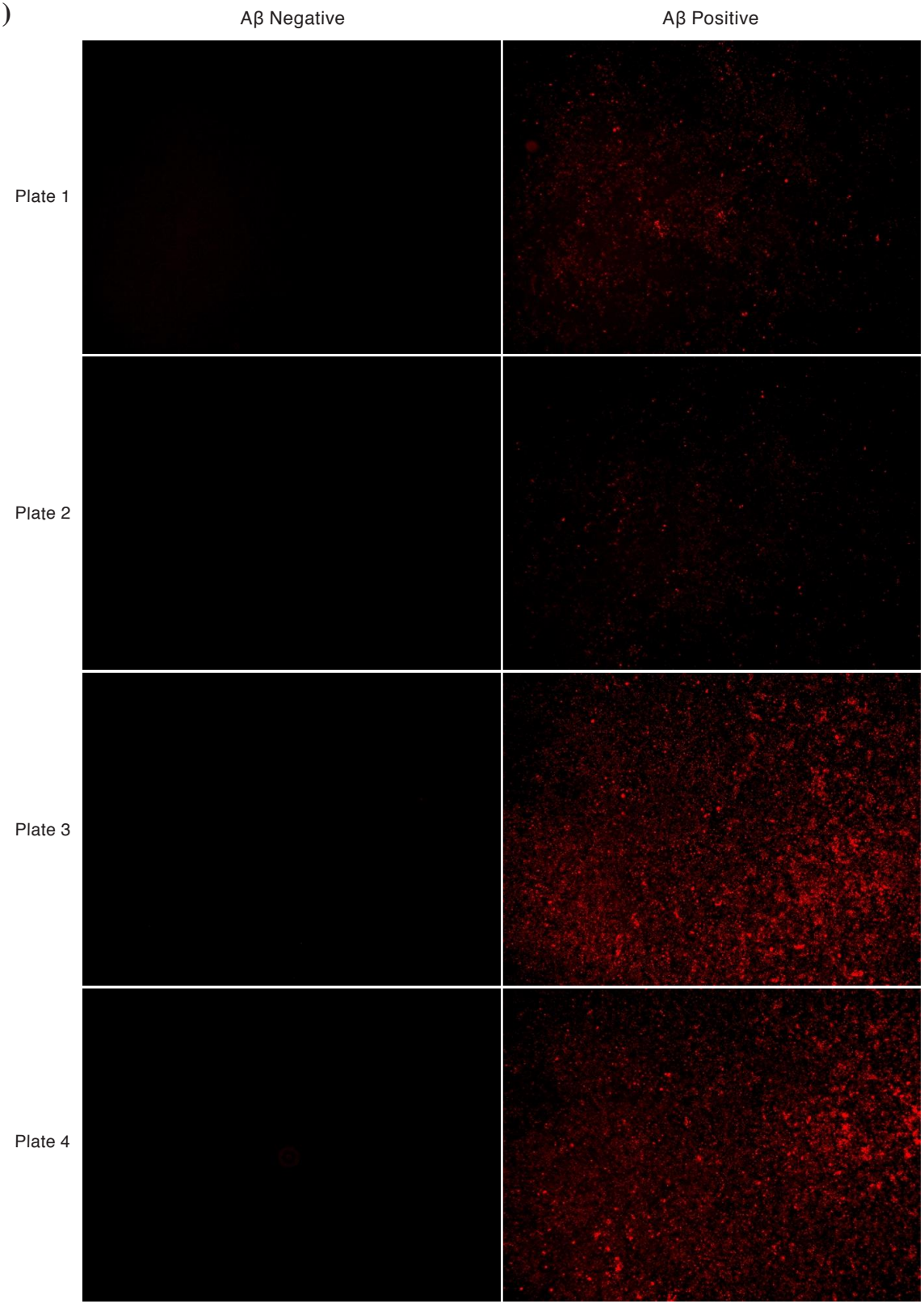

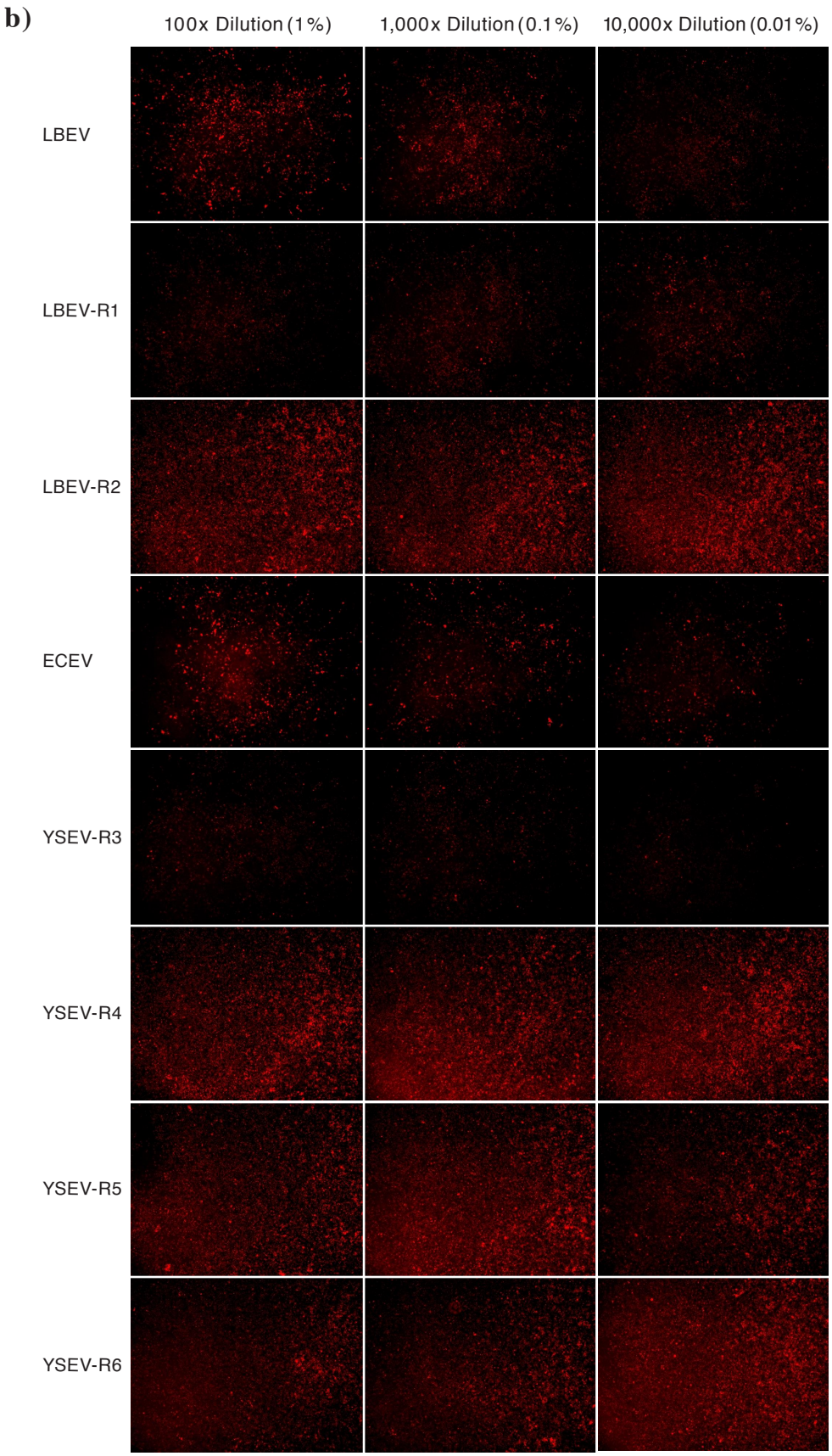


***Fig. 2.*** **Fluorescence imaging of cultured microglia.**

Images collected after washing of wells and replacing media post-Aβ and EV treatment. Red fluorescence indicates TAMRA-tagged Aβ which has been taken up by cells. **(a)** shows representative control wells from each plate. **(b)** shows representative sample wells for each EV treatment. Final fluorescence value was determined in relation to total cell area, as described in the methods section. Representative images. n = 4. EV, extracellular vesicle.

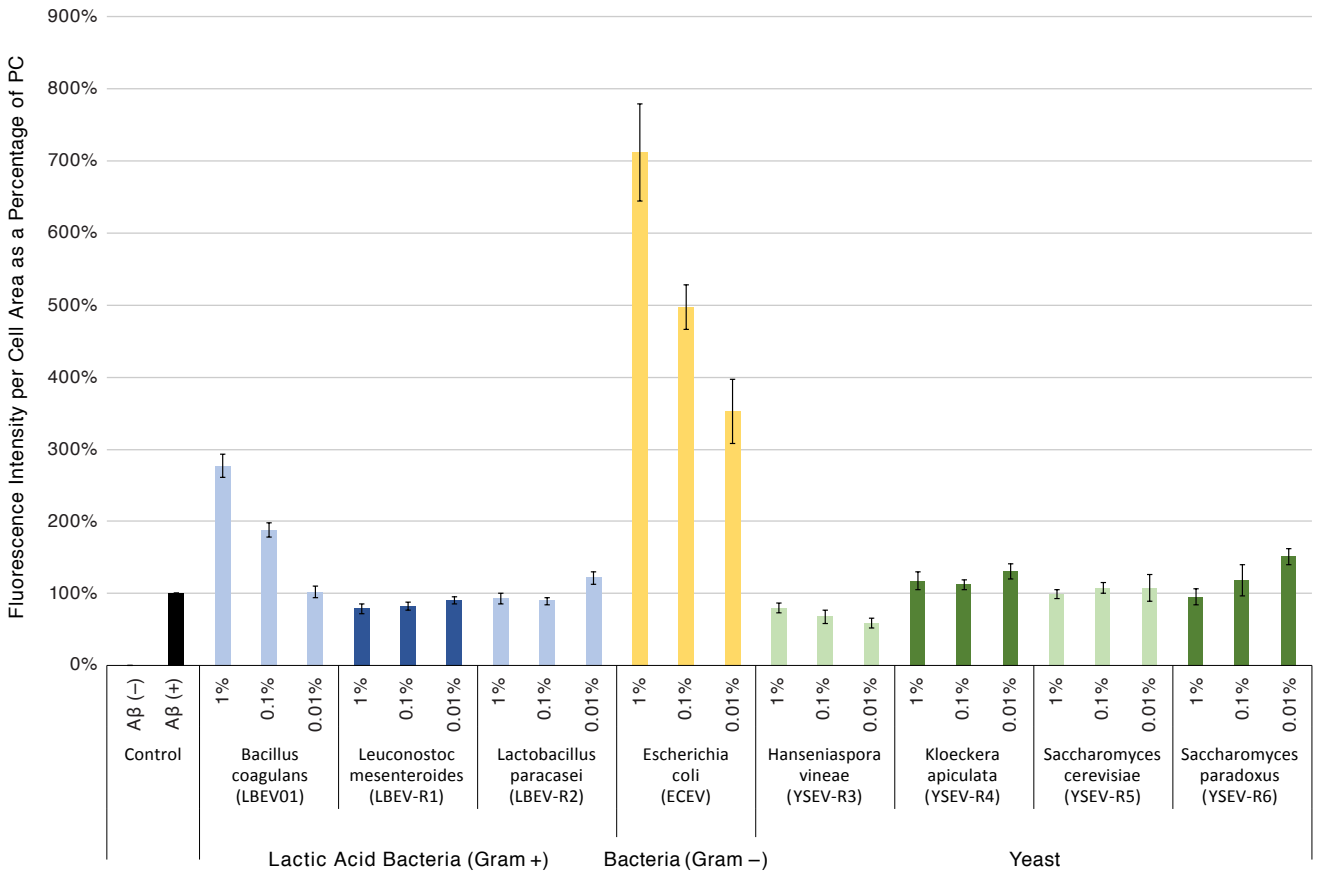


***Fig. 3.*** **Microglia Aβ phagocytosis potential.**

Phagocytosis potential of microglia treated with EVs indicated by fluorescence intensity of up-taken TAMRA-Aβ. Results expressed as % of fluorescence intensity in comparison with positive control wells of the same culture plate. n = 4. Bars indicate standard error of the mean. EVs, extracellular vesicles.

***Table 1. Aβ phagocytosis index: Plate 1.***

| Group (Plate 1) | FI (Integrated) | Area (Integrated) | FI/Area (Corrected) | Average | SEM | % NC | % PC |
|---|---|---|---|---|---|---|---|
| Negative Control (NC) Aβ (–) | 5,662 | 5,886,304 | 9.62E-04 | 2.57E-04 | 2.03E-04 | 100% | – |
| | 108 | 5,173,551 | 2.09E-05 | | | | |
| | 135 | 6,504,722 | 2.08E-05 | | | | |
| | 162 | 6,253,515 | 2.59E-05 | | | | |
| Positive Control (PC) Aβ (+) | 604,653 | 4,816,245 | 1.26E-01 | 1.51E-01 | 1.33E-02 | 58,529% | 100% |
| | 720,560 | 5,875,886 | 1.23E-01 | | | | |
| | 1,163,465 | 6,704,290 | 1.74E-01 | | | | |
| | 1,332,503 | 7,369,924 | 1.81E-01 | | | | |
| LBEV01 x100 Aβ (+) | 1,211,756 | 3,443,403 | 3.52E-01 | 4.17E-01 | 2.48E-02 | 161,981% | 277% |
| | 2,023,881 | 4,277,192 | 4.73E-01 | | | | |
| | 2,170,811 | 4,760,310 | 4.56E-01 | | | | |
| | 1,678,042 | 4,343,127 | 3.86E-01 | | | | |
| LBEV01 x1,000 Aβ (+) | 1,059,345 | 3,925,880 | 2.70E-01 | 2.83E-01 | 1.51E-02 | 110,009% | 188% |
| | 1,439,400 | 5,538,518 | 2.60E-01 | | | | |
| | 1,596,685 | 5,968,074 | 2.68E-01 | | | | |
| | 2,004,493 | 5,980,030 | 3.35E-01 | | | | |
| LBEV01 x10,000 Aβ (+) | 484,075 | 4,226,547 | 1.15E-01 | 1.54E-01 | 1.20E-02 | 59,892% | 102% |
| | 945,645 | 6,078,372 | 1.56E-01 | | | | |
| | 1,016,638 | 5,774,243 | 1.76E-01 | | | | |
| | 1,181,985 | 6,937,644 | 1.70E-01 | | | | |
| LBEV-R1 x100 Aβ (+) | 423,474 | 4,992,253 | 8.48E-02 | 1.19E-01 | 1.01E-02 | 46,089% | 79% |
| | 858,835 | 6,724,901 | 1.28E-01 | | | | |
| | 843,581 | 6,128,857 | 1.38E-01 | | | | |
| | 897,481 | 7,221,354 | 1.24E-01 | | | | |
| LBEV-R1 x1,000 Aβ (+) | 686,496 | 4,634,274 | 1.48E-01 | 1.24E-01 | 8.47E-03 | 48,279% | 82% |
| | 710,329 | 6,165,430 | 1.15E-01 | | | | |
| | 702,669 | 6,825,134 | 1.03E-01 | | | | |
| | 976,628 | 7,472,529 | 1.31E-01 | | | | |
| LBEV-R1 x10,000 Aβ (+) | 604,491 | 4,248,920 | 1.42E-01 | 1.38E-01 | 7.54E-03 | 53,478% | 91% |
| | 978,860 | 6,210,947 | 1.58E-01 | | | | |
| | 756,885 | 6,543,283 | 1.16E-01 | | | | |
| | 871,041 | 6,453,243 | 1.35E-01 | | | | |
| YSEV-R3 x100 Aβ (+) | 395,331 | 4,434,738 | 8.91E-02 | 1.20E-01 | 1.03E-02 | 46,600% | 80% |
| | 746,704 | 6,398,303 | 1.17E-01 | | | | |
| | 820,308 | 6,409,137 | 1.28E-01 | | | | |
| | 915,831 | 6,278,260 | 1.46E-01 | | | | |
| YSEV-R3 x1,000 Aβ (+) | 295,519 | 4,741,174 | 6.23E-02 | 1.03E-01 | 1.37E-02 | 39,831% | 68% |
| | 471,174 | 3,434,813 | 1.37E-01 | | | | |
| | 494,521 | 4,304,150 | 1.15E-01 | | | | |
| | 422,725 | 4,420,153 | 9.56E-02 | | | | |

***Table 2. Aβ phagocytosis index: Plate 2.***

| Group (Plate 2) | FI (Integrated) | Area (Integrated) | FI/Area (Corrected) | Average | SEM | % NC | % PC |
|---|---|---|---|---|---|---|---|
| Negative Control (NC) Aβ (–) | 5 | 5,825,113 | 8.58E-07 | 2.20E-04 | 1.83E-04 | 100% | – |
| | 28 | 7,062,462 | 3.96E-06 | | | | |
| | 132 | 6,300,474 | 2.10E-05 | | | | |
| | 5,839 | 6,845,136 | 8.53E-04 | | | | |
| Positive Control (PC) Aβ (+) | 264,613 | 6,015,738 | 4.40E-02 | 6.00E-02 | 1.01E-02 | 27,333% | 100% |
| | 264,740 | 5,136,753 | 5.15E-02 | | | | |
| | 259,160 | 5,192,431 | 4.99E-02 | | | | |
| | 554,611 | 5,852,807 | 9.48E-02 | | | | |
| YSEV-R3 x10,000 Aβ (+) | 163,736 | 6,176,329 | 2.65E-02 | 3.56E-02 | 4.21E-03 | 16,198% | 59% |
| | 196,163 | 5,547,236 | 3.54E-02 | | | | |
| | 168,509 | 5,372,446 | 3.14E-02 | | | | |
| | 321,880 | 6,555,047 | 4.91E-02 | | | | |
| ECEV x100 Aβ (+) | 1,499,848 | 3,359,325 | 4.46E-01 | 4.28E-01 | 4.03E-02 | 194,616% | 712% |
| | 1,685,811 | 4,572,057 | 3.69E-01 | | | | |
| | 2,379,460 | 4,320,337 | 5.51E-01 | | | | |
| | 1,483,269 | 4,307,932 | 3.44E-01 | | | | |
| ECEV x1,000 Aβ (+) | 800,189 | 3,292,172 | 2.43E-01 | 2.98E-01 | 1.84E-02 | 135,760% | 497% |
| | 1,459,591 | 4,890,546 | 2.98E-01 | | | | |
| | 1,496,563 | 4,904,041 | 3.05E-01 | | | | |
| | 1,756,677 | 5,071,715 | 3.46E-01 | | | | |
| ECEV x10,000 Aβ (+) | 519,033 | 3,350,703 | 1.55E-01 | 2.12E-01 | 2.68E-02 | 96,404% | 353% |
| | 1,103,828 | 5,097,519 | 2.17E-01 | | | | |
| | 875,578 | 4,886,988 | 1.79E-01 | | | | |
| | 1,525,473 | 5,143,644 | 2.97E-01 | | | | |

***Table 3. Aβ phagocytosis index: Plate 3.***

| Group (Plate 3) | FI (Integrated) | Area (Integrated) | FI/Area (Corrected) | Average | SEM | % NC | % PC |
|---|---|---|---|---|---|---|---|
| Negative Control (NC) Aβ (–) | 93 | 9,507,991 | 9.78E-06 | 7.92E-06 | 4.10E-06 | 100% | – |
| | 13 | 9,652,747 | 1.35E-06 | | | | |
| | 0 | 9,788,752 | 0.00E+00 | | | | |
| | 201 | 9,776,283 | 2.06E-05 | | | | |
| Positive Control (PC) Aβ (+) | 2,813,639 | 9,384,615 | 3.00E-01 | 3.89E-01 | 2.63E-02 | 4,915,385% | 100% |
| | 3,911,990 | 9,550,367 | 4.10E-01 | | | | |
| | 4,234,558 | 9,758,878 | 4.34E-01 | | | | |
| | 4,045,272 | 9,765,609 | 4.14E-01 | | | | |
| LBEV-R2 x100 Aβ (+) | 3,563,642 | 9,328,617 | 3.82E-01 | 3.64E-01 | 2.83E-02 | 4,591,817% | 93% |
| | 3,085,479 | 9,726,664 | 3.17E-01 | | | | |
| | 2,991,194 | 9,725,061 | 3.08E-01 | | | | |
| | 4,360,414 | 9,727,690 | 4.48E-01 | | | | |
| LBEV-R2 x1,000 Aβ (+) | 2,806,045 | 9,549,565 | 2.94E-01 | 3.49E-01 | 1.98E-02 | 4,400,471% | 90% |
| | 3,033,669 | 9,245,821 | 3.28E-01 | | | | |
| | 3,730,598 | 9,657,427 | 3.86E-01 | | | | |
| | 3,620,210 | 9,374,550 | 3.86E-01 | | | | |
| LBEV-R2 x10,000 Aβ (+) | 4,131,068 | 9,459,814 | 4.37E-01 | 4.73E-01 | 3.53E-02 | 5,975,338% | 122% |
| | 5,769,672 | 9,788,592 | 5.89E-01 | | | | |
| | 4,543,545 | 9,777,918 | 4.65E-01 | | | | |
| | 3,936,952 | 9,777,245 | 4.03E-01 | | | | |
| YSEV-R4 x100 Aβ (+) | 3,282,142 | 9,396,700 | 3.49E-01 | 4.58E-01 | 4.83E-02 | 5,784,151% | 118% |
| | 4,335,172 | 9,588,255 | 4.52E-01 | | | | |
| | 5,824,778 | 9,508,761 | 6.13E-01 | | | | |
| | 3,856,215 | 9,205,786 | 4.19E-01 | | | | |
| YSEV-R4 x1,000 Aβ (+) | 3,895,491 | 9,484,624 | 4.11E-01 | 4.37E-01 | 2.66E-02 | 5,517,974% | 112% |
| | 4,919,042 | 9,722,208 | 5.06E-01 | | | | |
| | 4,519,760 | 9,703,136 | 4.66E-01 | | | | |
| | 3,588,706 | 9,803,754 | 3.66E-01 | | | | |
| YSEV-R4 x10,000 Aβ (+) | 4,138,259 | 9,429,779 | 4.39E-01 | 5.10E-01 | 4.17E-02 | 6,440,278% | 131% |
| | 5,383,515 | 9,714,067 | 5.54E-01 | | | | |
| | 6,013,773 | 9,622,456 | 6.25E-01 | | | | |
| | 4,125,694 | 9,758,654 | 4.23E-01 | | | | |

***Table 4. Aβ phagocytosis index: Plate 4.***

| Group (Plate 4) | FI (Integrated) | Area (Integrated) | FI/Area (Corrected) | Average | SEM | % NC | % PC |
|---|---|---|---|---|---|---|---|
| Negative Control (NC) Aβ (–) | 24 | 9,417,310 | 2.55E-06 | 1.86E-05 | 8.82E-06 | 100% | – |
| | 437 | 9,154,948 | 4.77E-05 | | | | |
| | 66 | 9,450,679 | 6.98E-06 | | | | |
| | 157 | 9,202,933 | 1.71E-05 | | | | |
| Positive Control (PC) Aβ (+) | 2,391,344 | 9,263,451 | 2.58E-01 | 4.12E-01 | 5.43E-02 | 2,218,776% | 100% |
| | 3,413,630 | 9,413,528 | 3.63E-01 | | | | |
| | 4,688,823 | 8,925,858 | 5.25E-01 | | | | |
| | 4,470,963 | 8,888,002 | 5.03E-01 | | | | |
| YSEV-R5 x100 Aβ (+) | 2,900,540 | 8,218,362 | 3.53E-01 | 4.09E-01 | 2.67E-02 | 2,199,345% | 99% |
| | 3,614,128 | 9,181,938 | 3.94E-01 | | | | |
| | 3,495,214 | 8,930,378 | 3.91E-01 | | | | |
| | 4,548,559 | 9,156,711 | 4.97E-01 | | | | |
| YSEV-R5 x1,000 Aβ (+) | 4,418,553 | 8,788,282 | 5.03E-01 | 4.44E-01 | 3.01E-02 | 2,387,125% | 108% |
| | 4,510,538 | 9,432,600 | 4.78E-01 | | | | |
| | 3,130,062 | 9,076,384 | 3.45E-01 | | | | |
| | 4,016,462 | 8,956,822 | 4.48E-01 | | | | |
| YSEV-R5 x10,000 Aβ (+) | 1,610,305 | 8,600,189 | 1.87E-01 | 4.42E-01 | 7.64E-02 | 2,381,207% | 107% |
| | 4,072,978 | 8,818,734 | 4.62E-01 | | | | |
| | 4,839,843 | 8,665,964 | 5.58E-01 | | | | |
| | 5,058,385 | 8,996,473 | 5.62E-01 | | | | |
| YSEV-R6 x100 Aβ (+) | 2,052,659 | 8,411,680 | 2.44E-01 | 3.92E-01 | 4.68E-02 | 2,111,455% | 95% |
| | 4,319,855 | 9,027,758 | 4.79E-01 | | | | |
| | 3,375,537 | 8,882,329 | 3.80E-01 | | | | |
| | 4,196,109 | 8,989,261 | 4.67E-01 | | | | |
| YSEV-R4 x1,000 Aβ (+) | 1,975,823 | 8,409,340 | 2.35E-01 | 4.88E-01 | 8.75E-02 | 2,624,358% | 118% |
| | 3,844,901 | 9,150,365 | 4.20E-01 | | | | |
| | 6,151,844 | 8,985,158 | 6.85E-01 | | | | |
| | 5,264,390 | 8,619,454 | 6.11E-01 | | | | |
| YSEV-R4 x10,000 Aβ (+) | 5,560,499 | 8,481,013 | 6.56E-01 | 6.23E-01 | 4.80E-02 | 3,355,494% | 151% |
| | 6,989,858 | 9,202,100 | 7.60E-01 | | | | |
| | 5,079,973 | 8,776,134 | 5.79E-01 | | | | |
| | 4,440,652 | 8,882,746 | 5.00E-01 | | | | |

NC, negative control (Aβ –); PC, positive control (Aβ +); FI, fluorescence intensity; SEM , standard error of the mean; LBEV01, *Bacillus coagulans* lilac-01; LBEV-R1, *Lactobacillus paracasei*; LBEV-R2, *Leuconostoc mesenteroides*; ECEV, *Escherichia coli* DH5α; YSEV-R3, *Hanseniaspora vineae*; YSEV-R4, *Kloeckera / Hanseniaspora apiculate*; YSEV-R5, *Saccharomyces cerevisiae*; YSEV-R6, *Saccharomyces paradoxus*.

## *Discussion*

Large differences in the magnitude and direction of Aβ phagocytosis were observed in the results between difference source species. Strain-specific variations in EV contents and vesicle surface composition will likely account for the difference in results. EV contents and morphology are complex and poorly described. However, some potential points of interest can be hypothesized based on known characteristics of the tested EVs.

### *Lactic acid bacteria and gram + EVs*

From the selection of Gram + EVs, *B. coagulans* lilac-01 stood out by exhibiting a substantial dose-dependent enhancement of microglia Aβ phagocytosis. The EVs of gram + bacteria remain poorly understood, both in terms of their composition and the mechanisms involved in their production. However, *B. coagulans* lilac-01 EVs have been previously reported to enhance microglia survival and contain cardiolipin and its precursor phosphatidylglycerol[36].

Cardiolipin is a protein with a role in mitochondrial functioning, and also functions as a signaling molecule in the positive feedback loop regulating phagocytoses after uptake of Aβ microglia, enhancing phagocytosis[37,38]. Cardiolipin levels in the brain have been reported to decrease with age, and impairment of cardiolipin by lipid oxidation is thought to play a role in mitochondrial dysfunction in Parkinson's disease[39]. Cardiolipin rich EVs like those of *B. coagulans* lilac-01 may be able to supplement falling cardiolipin levels in the CNS and upregulate clearance of neurodegenerative neural plaques by enacting their signaling role in microglia phagocytosis.

*L. paracasei* is reported to improve cognitive functioning via anti-inflammatory effects, and ameliorate age-related gut permeability [40]. However, microglia phagocytosis was only minimally affected by *L. paracasei* EV treatment in this study.

### *E. coli EVs*

The greatest enhancement in Aβ phagocytosis was observed in the ECEV treatment, with a result of 712% increased Aβ uptake in relation to the positive control. The DH5α strain of *E. coli* in particular is an engineered strain developed for ease of plasmid insertion and transformation. It lacks the virulence factors found in pathogenic *E. coli* strains [41]. Thus, it has potential for use in the production of probiotic EVs, as bacterial virulence factors are propagated by EVs [42]. More generally, *E. coli* is distinguished from the other bacterial EVs tested by being a gram – bacterium. Gram–species feature an outer membrane containing LPS as a major structural component, and their peptidoglycan cell wall exists between the inner and outer lipid membranes. Their EVs are primarily produced by budding of the outer membrane and are thus rich in LPS content.

LPS is an immunomodulatory molecule consisting of a conserved lipid unit (Lipid A), a core polysaccharide, and a variable number of O-antigen polysaccharide-chain tails [43]. The composition of LPS and the resulting strength of immune reaction vary greatly between strains and species. LPS induces an immune response by activation of macrophage Toll-like receptors (TLRs) in a complex with LPS-binding protein and CD14. The LPS of *E. coli* DH5α lacks the O-antigen tails, retaining its core polysaccharide and the Lipid A unit which interfaces with TLR-4 [41].

TLR activation is necessary for Aβ phagocytosis by microglia, and operates by a similar mechanistic pathway as LPS immune-response: coupling of CD14 to TLR-2 and TLR-4 is necessary for Aβ phagocytosis [44] as well as the inflammatory response to LPS [45]. Impairment of TLR-4 inhibits microglia phagocytosis [46] and has been demonstrated to cause increased Aβ deposition in mice [47]. Conversely, activation of TLR-2 enhances phagocytosis [48, 49]. Reports of the effects of LPS on phagocytotic capacity are mixed. Some reports indicate increased phagocytosis from LPS stimulation [50], while *E. coli* O111:B4 (L4391) was found to impair microglia autophagy and Aβ phagocytotic capacity [51]. These differences may be due to strain-dependent variations in LPS structure.

The large increase in microglia Aβ phagocytosis by ECEV treatment is speculated to be due to the activation of TLRs by LPS upregulating phagocytosis. However, LPS is also suspected to play a contributory role in neurodegenerative disease [15]. High circulating levels of LPS are associated with AD severity and contribute to chronic systemic inflammation. The pro-inflammatory function of microglia accelerates tissue damage via the production of inflammatory cytokines and reactive oxygen species [52], while overactive pathogenic phagocytosis leads to the destruction of viable neurons, contributing to neurodegeneration [53, 54]. While systemic LPS challenge induces microglia activation [55], LPS itself penetrates poorly across the BBB, with only 0.025% uptake [56]; this likely does not reach high enough concentrations to exert effects on CNS resident cells directly without EV carriers under normal conditions outside of infection. High dosages of LPS in the blood, such as those during infection, cause damage to the BBB and increase its permeability [57].

Further study is necessary to evaluate the effects of LPS in the CNS, particularly forms like those produced by *E. coli* DH5α which may have altered immunomodulatory effects in comparison to common LPS variants. Acute LPS treatment may be neuroprotective, while chronic exposure ultimately worsens Aβ clearance. If these risks can be mitigated, LPS-containing EVs may be an incredibly powerful tool for enhancing the functioning of microglia and clearing Aβ from the cerebral environment.

### *Yeast EVs*

EVs derived from probiotic yeast strains failed to demonstrate phagocytotic enhancing effects to the same degree as *B. coagulans* lilac-01 and *E. coli* DH5α. Minimal phagocytosis enhancement and inhibition were observed, varying between species. EVs from the currently tested strains lack previous testing data, and it is difficult to speculate about the causes of their effects on microglia.

*S. cerevisiae* extracts have been shown to reduce LPS-induced inflammation in BV2 microglia [58] and supplementation has led to reduced Aβ accumulation and neuroinflammation in animal models of AD [59]. Additionally, β-glucan produced by *S. cerevisiae* has demonstrated immunomodulatory effects on microglia in a mouse stress-induced depression model [60]. However, in the current study *S. cerevisiae* failed to induce any major change in uptake of Aβ by microglia.

In a broader context, EVs from other fungal species have demonstrated immunomodulatory effects [61], and unsurprisingly the effects differ between species. *P. brasiliensis* EVs induce M1 polarization in macrophages [62], while *H. capsulatom* EVs inhibit phagocytosis [63] and *E. dermatitides* exerts a neurotoxic effect [64]. The effect of any strain's EVs on microglia functioning are difficult to predict, although probiotic yeast strains are less likely to propagate virulence factors in their EVs.

Fungal cells are characterized by a cell wall of which α- and β-glucans are major components. β-glucan is also found in EVs produced by yeasts which is endocytosed by immune cells, activating TLR-2 [65]. The possibility of β-glucan activating microglia without inducing cytokine production [66] is a promising pathway for improvement of Aβ clearance while avoiding the negative effects of the inflammatory response in the CNS. However, soluble α-glucan and β-glucan have also been shown to inhibit phagocytosis of glucan-containing fungal cells [67, 68]. EVs containing α- and β-Glucans may competitively inhibit Aβ clearance despite otherwise enhancing phagocytosis, which may explain the observed result of lower concentrations of yeast EVs resulting in higher Aβ phagocytosis in this experiment.

## *Conclusions*

Probiotic EVs possess a promising potential as therapeutics in the treatment of neurodegenerative diseases like Alzheimer's disease by improving microglia function

and assisting in the clearance of Aβ from the CNS by enhancing phagocytosis. We have identified two strains of probiotic bacteria whose EVs enhanced Aβ phagocytosis by BV2 microglia *in vitro: B. coagulans* lilac-01, and *E. coli* DH5α. These results show the diversity of bacterial products and their effects on human health. While bacterial molecular patterns are generally associated with neurodegenerative disease and systemic inflammation, probiotic strains and their products are a potent source of beneficial compounds.

By identifying the causative agents carried by probiotic EVs, treatments may be developed to deliver therapeutics across the BBB to alleviate symptoms and halt progression of neurodegenerative diseases. Engineering EVs for targeted treatments across the BBB and for improving microglia functioning are promising targets in the fight against AD and other age-related causes of cognitive decline.

## Research grants

This research was supported by a Grant-in-Aid for Scientific Research from the Ministry of Education, Culture, Sports, Science and Technology (KAKEN 23K10882).

## Conflict of Interest Declaration

None.

## Reference

1) Naj AC, Schellenberg GD, Alzheimer's Disease Genetics Consortium (ADGC). Genomic variants, genes, and pathways of Alzheimer's disease: An overview. *Am J Med Genet B Neuropsychiatr Genet*. 2017; 174: 5-26.
2) McQuade A, Blurton-Jones M. Microglia in Alzheimer's disease: Exploring how genetics and phenotype influence risk. *J Mol Biol*. 2019; 431: 1805-1817.
3) Podleśny-Drabiniok A, Marcora E, Goate AM. Microglial phagocytosis: A disease-associated process emerging from Alzheimer's disease genetics. *Trends Neurosci*. 2020; 43: 965-979.
4) Zhao N, Chen QG, Chen X, et al. Intestinal dysbiosis mediates cognitive impairment via the intestine and brain NLRP3 inflammasome activation in chronic sleep deprivation. *Brain Behav Immun*. 2023; 108: 98-117.
5) Jia M, Fan Y, Ma Q, et al. Gut microbiota dysbiosis promotes cognitive impairment via bile acid metabolism in major depressive disorder. *Transl Psychiatry*. 2024; 14: 503.
6) Kelly JR, Kennedy PJ, Cryan JF, et al. Breaking down the barriers: The gut microbiome, intestinal permeability and stress-related psychiatric disorders. *Front Cell Neurosci*. 2015; 9: 392.
7) Pei Y, Lu Y, Li H, et al. Gut microbiota and intestinal barrier function in subjects with cognitive impairments: A cross-sectional study. *Front Aging Neurosci*. 2023; 15: 1174599.
8) Scheurink TAW, Borkent J, Gangadin SS, et al. Association between gut permeability, brain volume, and cognition in healthy participants and patients with schizophrenia spectrum disorder. *Brain Behav*. 2023; 13: e3011.
9) Saji, N., Niida, S., Murotani, K. et al. Analysis of the relationship between the gut microbiome and dementia: A cross-sectional study conducted in Japan. *Sci Rep*. 2019; 9: 1008.
10) Vogt NM, Kerby RL, Dill-McFarland KA, et al. Gut microbiome alterations in Alzheimer's disease. *Sci Rep*. 2017; 7: 13537.
11) Ferreiro AL, Choi J, Ryou J, et al. Gut microbiome composition may be an indicator of preclinical Alzheimer's disease. *Sci Transl Med*. 2023; 15: eabo2984.
12) Gofton T, Young G. Sepsis-associated encephalopathy. *Nat Rev Neurol*. 2012; 8: 557-566.
13) Sekino N, Selim M, Shehadah A. Sepsis-associated brain injury: Underlying mechanisms and potential therapeutic strategies for acute and long-term cognitive impairments. *J Neuroinflammation*. 2022; 19: 101.
14) Zhang R, Miller RG, Gascon R, et al. Circulating endotoxin and systemic immune activation in sporadic amyotrophic lateral sclerosis (sALS). *J Neuroimmunol*. 2009; 206: 121-124.
15) Brown GC, Heneka MT. The endotoxin hypothesis of Alzheimer's disease. *Mol Neurodegener*. 2024; 19: 30.
16) Inaba T, Yamashiro K, Kurita N, et al. Microbial lipopolysaccharide-induced inflammation contributes to cognitive impairment and white matter lesion progression in diet-induced obese mice with chronic cerebral hypoperfusion. *CNS Neurosci Ther*. 2023; 29 Suppl 1: 200-212.
17) Dominy SS, Lynch C, Ermini F, et al. Porphyromonas gingivalis in Alzheimer's disease brains: Evidence for disease causation and treatment with small-molecule inhibitors. *Sci Adv*. 2019; 5: eaau3333.
18) Beydoun MA, Beydoun HA, Hossain S, et al. Clinical and bacterial markers of periodontitis and their association with incident all-cause and Alzheimer's disease dementia in a large national survey. *J Alzheimers Dis*. 2020; 75: 157-172.
19) Jones EJ, Booth C, Fonseca S, et al. The uptake, trafficking, and biodistribution of *Bacteroides thetaiotaomicron* generated outer membrane vesicles. *Front Microbiol*. 2020; 11: 57.
20) Schaack B, Hindré T, Quansah N, et al. Microbiota-derived extracellular vesicles detected in human blood from healthy donors. *Int J Mol Sci*. 2022; 23: 13787.
21) Ou Z, Situ B, Huang X, et al. Single-particle analysis of circulating bacterial extracellular vesicles reveals their biogenesis, changes in blood and links to intestinal barrier. *J Extracell Vesicles*. 2023; 12: e12395.
22) Tulkens J, Vergauwen G, Van Deun J, et al. Increased levels of systemic LPS-positive bacterial extracellular vesicles in patients with intestinal barrier dysfunction. *Gut*. 2020; 69: 191-193.

23) Banks WA, Sharma P, Bullock KM, et al. Transport of extracellular vesicles across the blood-brain barrier: Brain pharmacokinetics and effects of inflammation. *Int J Mol* Sci. 2020; 21: 4407.
24) Liu Y, Defourny KAY, Smid EJ, et al. Gram-positive bacterial extracellular vesicles and their impact on health and disease. *Front Microbiol*. 2018; 9: 1502.
25) Hosseini-Giv N, Basas A, Hicks C, et al. Bacterial extracellular vesicles and their novel therapeutic applications in health and cancer. *Front Cell Infect Microbiol*. 2022; 12: 962216.
26) Yonei Y, Haasbroek K, Otaka S, et al. Actions of mesenchymal stem cell secretome on microglia amyloid-β uptake. *Glycative Stress Res*. 2024; 11: 192-203.
27) Santamaria G, Brandi E, Vitola P, et al. Intranasal delivery of mesenchymal stem cell secretome repairs the brain of Alzheimer's mice. *Cell Death Differ*. 2021; 28: 203-218.
28) Xie X, Song Q, Dai C, et al. Clinical safety and efficacy of allogenic human adipose mesenchymal stromal cells-derived exosomes in patients with mild to moderate Alzheimer's disease: a phase I/II clinical trial. *Gen Psychiatr*. 2023; 36: e101143.
29) Morita Y, Izawa H, Ohga H, et al. Safety and clinical efficacy on intranasal administration of mesenchymal stem cell-derived secretome in patients with Alzheimer's disease and its future prospect. *Glycative Stress Res*. 2024; 11: 103-110.
30) Yamasaki-Yashiki S, Miyoshi Y, Nakayama T, et al. IgA-enhancing effects of membrane vesicles derived from Lactobacillus sakei subsp. sakei NBRC15893. *Biosci Microbiota Food Health*. 2019; 38: 23-29.
31) Fábrega MJ, Rodríguez-Nogales A, Garrido-Mesa J, et al. Intestinal anti-inflammatory effects of outer membrane vesicles from *Escherichia coli* Nissle 1917 in DSS-experimental colitis in mice. *Front Microbiol*. 2017; 8: 1274.
32) Seo MK, Park EJ, Ko SY, et al. Therapeutic effects of kefir grain Lactobacillus-derived extracellular vesicles in mice with 2,4,6-trinitrobenzene sulfonic acid-induced inflammatory bowel disease. *J Dairy Sci*. 2018; 101: 8662-8671.
33) Park KS, Lee J, Jang SC, et al. Pulmonary inflammation induced by bacteria-free outer membrane vesicles from *Pseudomonas aeruginosa*. *Am J Respir Cell Mol Biol*. 2013; 49: 637-645.
34) Choi HI, Choi JP, Seo J, et al. *Helicobacter pylori*-derived extracellular vesicles increased in the gastric juices of gastric adenocarcinoma patients and induced inflammation mainly via specific targeting of gastric epithelial cells. *Exp Mol Med*. 2017; 49: e330.
35) Cosmo Bio Co. Ltd. Primary Microglia Culture Kit (SD rat), Code No. MGSD. Attachment. https://search.cosmobio.co.jp/cosmo_search_p/search_gate2/docs/PMC_/MGSD.20181218.pdf. Accessed at November 30, 2024. (in Japanese)
36) Minamida K, Taira T, Sasaki M, et al. Extracellular vesicles of Weizmannia coagulans lilac-01 reduced cell death of primary microglia and increased mitochondrial content in dermal fibroblasts *in vitro*. *Biosci Biotechnol Biochem*. 2024; 88: 333-343.
37) Wenzel TJ, Ranger AL, McRae SA, et al. Extracellular cardiolipin modulates microglial phagocytosis and cytokine secretion in a toll-like receptor (TLR) 4-dependent manner. *J Neuroimmunol*. 2021; 353: 577496.
38) Wenzel TJ, Murray TE, Noyovitz B, et al. Cardiolipin released by microglia can act on neighboring glial cells to facilitate the uptake of amyloid-β (1-42). *Mol Cell Neurosci*. 2023; 124: 103804.
39) Ruggiero FM, Cafagna F, Petruzzella V, et al. Lipid composition in synaptic and nonsynaptic mitochondria from rat brains and effect of aging. *J Neurochem*. 1992; 59: 487-491.
40) Wang S, Ahmadi S, Nagpal R, et al. Lipoteichoic acid from the cell wall of a heat killed *Lactobacillus paracasei* D3-5 ameliorates aging-related leaky gut, inflammation and improves physical and cognitive functions: From *C. elegans* to mice. *Geroscience*. 2020; 42: 333-352.
41) Chart H, Smith HR, La Ragione RM, et al. An investigation into the pathogenic properties of *Escherichia coli* strains BLR, BL21, DH5α and EQ1. *J Appl Microbiol*. 2000; 89: 1048-1058.
42) Hong J, Dauros-Singorenko P, Whitcombe A, et al. Analysis of the *Escherichia coli* extracellular vesicle proteome identifies markers of purity and culture conditions. *J Extracell Vesicles*. 2019; 8: 1632099.
43) Bertani B, Ruiz N. Function and biogenesis of lipopolysaccharides. *EcoSal Plus*. 2018; 8: 10.1128/ecosalplus. ESP-0001-2018.
44) Reed-Geaghan EG, Savage JC, Hise AG, et al. CD14 and toll-like receptors 2 and 4 are required for fibrillar A{beta}-stimulated microglial activation. *J Neurosci*. 2009; 29: 11982-11992.
45) Tsukamoto H, Takeuchi S, Kubota K, et al. Lipopolysaccharide (LPS)-binding protein stimulates CD14-dependent Toll-like receptor 4 internalization and LPS-induced TBK1-IKKε-IRF3 axis activation. *J Biol Chem*. 2018; 293: 10186-10201.
46) Rajbhandari L, Tegenge MA, Shrestha S, et al. Toll-like receptor 4 deficiency impairs microglial phagocytosis of degenerating axons. *Glia*. 2014; 62: 1982-1991.
47) Song M, Jin J, Lim JE, et al. TLR4 mutation reduces microglial activation, increases Aβ deposits and exacerbates cognitive deficits in a mouse model of Alzheimer's disease. *J Neuroinflammation*. 2011; 8: 92.
48) Chen K, Iribarren P, Hu J, et al. Activation of Toll-like receptor 2 on microglia promotes cell uptake of Alzheimer disease-associated amyloid β peptide. *J Biol Chem*. 2006; 281: 3651-3659.
49) Ribes S, Adam N, Ebert S, et al. The viral TLR3 agonist poly(I:C) stimulates phagocytosis and intracellular killing of *Escherichia coli* by microglial cells. *Neurosci Lett*. 2010; 482: 17-20.
50) Hide I, Shiraki H, Masuda A, et al. $P2Y_2$ receptor mediates dying cell removal via inflammatory activated microglia. *J Pharmacol Sci*. 2023; 153: 55-67.
51) Lee JW, Nam H, Kim LE, et al. TLR4 (toll-like receptor 4) activation suppresses autophagy through inhibition of FOXO3 and impairs phagocytic capacity of microglia. *Autophagy*. 2019; 15: 753-770.
52) Hansen DV, Hanson JE, Sheng M. Microglia in Alzheimer's disease. *J Cell Biol*. 2018; 217: 459-472.
53) Brown GC, Neher JJ. Microglial phagocytosis of live neurons. *Nat Rev Neurosci*. 2014; 15: 209-216.
54) Wang K, Li J, Zhang Y, et al. Central nervous system diseases related to pathological microglial phagocytosis. *CNS Neurosci Ther*. 2021; 27: 528-539.

55) Hoogland ICM, Westhoff D, Engelen-Lee JY, et al. Microglial activation after systemic stimulation with lipopolysaccharide and *Escherichia coli*. *Front Cell Neurosci*. 2018; 12: 110.
56) Banks WA, Robinson SM. Minimal penetration of lipopolysaccharide across the murine blood-brain barrier. *Brain Behav Immun*. 2010; 24: 102-109.
57) Banks WA, Gray AM, Erickson MA, et al. Lipopolysaccharide-induced blood-brain barrier disruption: Roles of cyclooxygenase, oxidative stress, neuroinflammation, and elements of the neurovascular unit. *J Neuroinflammation*. 2015; 12: 223.
58) Armeli F, Mengoni B, Maggi E, et al. Milmed yeast alters the LPS-induced M1 microglia cells to form M2 anti-inflammatory phenotype. *Biomedicines*. 2022; 10: 3116.
59) Neta FI, de Souza FES, Batista AL, et al. Effects of supplementation with probiotics in experimental models of Alzheimer's disease: A systematic review of animal experiments. *Curr Alzheimer Res*. 2022; 19: 188-201.
60) Zhao C, Shi R, Lu X, et al. Obligatory role of microglia-mobilized hippocampal CREB-BDNF signaling in the prophylactic effect of β-glucan on chronic stress-induced depression-like behaviors in mice. *Eur J Pharmacol*. 2024; 964: 176288.
61) Oliveira DL, Freire-de-Lima CG, Nosanchuk JD, et al. Extracellular vesicles from *Cryptococcus neoformans* modulate macrophage functions. *Infect Immun*. 2010; 78: 1601-1609.
62) da Silva TA, Roque-Barreira MC, Casadevall A, et al. Extracellular vesicles from *Paracoccidioides brasiliensis* induced M1 polarization *in vitro*. *Sci Rep*. 2016; 6: 35867.
63) Baltazar LM, Zamith-Miranda D, Burnet MC, et al. Concentration-dependent protein loading of extracellular vesicles released by *Histoplasma capsulatum* after antibody treatment and its modulatory action upon macrophages. *Sci Rep*. 2018; 8: 8065.
64) Lavrin T, Konte T, Kostanjšek R, et al. The neurotropic black yeast *Exophiala dermatitidis* induces neurocytotoxicity in neuroblastoma cells and progressive cell death. *Cells*. 2020; 9: 963.
65) Higuchi A, Morishita M, Nagata R, et al. Functional characterization of extracellular vesicles from baker's yeast *Saccharomyces cerevisiae* as a novel vaccine material for immune cell maturation. *J Pharm Sci*. 2023; 112: 525-534.
66) Shah VB, Huang Y, Keshwara R, et al. β-glucan activates microglia without inducing cytokine production in Dectin-1-dependent manner. *J Immunol*. 2008; 180: 2777-2785.
67) Janusz MJ, Austen KF, Czop JK. Isolation of soluble yeast β-glucans that inhibit human monocyte phagocytosis mediated by β-glucan receptors. *J Immunol*. 1986; 137: 3270-3276.
68) Bittencourt VC, Figueiredo RT, da Silva RB, et al. An alpha-glucan of *Pseudallescheria boydii* is involved in fungal phagocytosis and Toll-like receptor activation. *J Biol Chem*. 2006; 281: 22614-22623.